Published in final edited form as:
Brain Res. 2010 February 2; 1312C: 54–66. doi:10.1016/j.brainres.2009.11.042.

Optical tracking of phenotypically diverse individual synapses on solitary tract nucleus neurons

Y.-H. Jin[&,@], **E.A. Cahill**[#,@,%], **L.G. Fernandes**[*], **X. Wang**[#], **W. Chen**[#], **S.M. Smith**[#], and **M.C. Andresen**

Department of Physiology and Pharmacology, Oregon Health & Science University, Portland, Oregon USA 97239-3098

[#] Division of Pulmonary and Critical Care Medicine, Oregon Health & Science University, Portland, Oregon USA 97239-3098

[&] Department of Physiology, Kyung Hee University, Seoul 130-701, Korea

Abstract

The solitary tract nucleus (NTS) is the termination site for cranial visceral afferents - peripheral primary afferent neurons which differ by phenotype (e.g. myelinated and unmyelinated). These afferents have very uniform glutamate release properties calculated by variance mean analysis. In the present study, we optical measured the inter-terminal release properties across individual boutons by assessing vesicle membrane turnover with the dye FM1-43. Single neurons were mechanically micro-harvested from medial NTS without enzyme treatment. The TRPV1 agonist capsaicin (CAP, 100 nM) was used to identify afferent, CAP-sensitive terminals arising from unmyelinated afferents. Isolated NTS neurons retained both glutamatergic and inhibitory terminals that generated EPSCs and IPSCs, respectively. Visible puncta on the neurons were stained positively with monoclonal antibody for synaptophysin, a presynaptic marker. Elevating extracellular K^+ concentration to 10 mM increased synaptic release measured at individual terminals by FM1-43. Within single neurons, CAP destained some but not other individual terminals. FM1-43 positive terminals that were resistant to CAP could be destained with K^+ solution. Individual terminals responded to depolarization with similar vesicle turnover kinetics. Thus, vesicular release was relatively homogenous across individual release sites. Surprisingly, conventionally high K^+ concentrations (>50 mM) produced erratic synaptic responses and at 90 mM K^+ overt neuron swelling – results that suggest precautions about assuming consistent K^+ responses in all neurons. The present work demonstrates remarkably uniform glutamate release between individual unmyelinated terminals and suggests that the homogeneous EPSC release properties of solitary tract afferents result from highly uniform release properties across multiple contacts on NTS neurons.

To whom correspondence should be sent: Dr. Michael C. Andresen, Department of Physiology and Pharmacology, Oregon Health & Science University, Portland, Oregon 97239-3098, Voice: (503) 494-5831, FAX: (503) 494-4352, andresen.ohsu@gmail.com.
[@]Contributed equally to this work
[%]Albert Einstein College of Medicine, 1300 Morris Park Ave, Bronx,NY 10461
[*]Universidade Federal de Ouro Preto, Instituto de Ciências Exatas e Biológicas, Campus Universitário - ICEB II, Sala 39, Ouro Preto - MG – Brasil.
Senior Editor: Alan F. Sved

Keywords

TRPV1; capsaicin; glutamatergic; GABAergic; vesicle turnover; primary afferent

1. INTRODUCTION

The release of neurotransmitter during synaptic transmission depends on a highly regulated series of events within the presynaptic terminal. Small CNS synaptic terminals are difficult to record from directly so that presynaptic mechanisms are most often assessed indirectly using electrophysiological measures of postsynaptic events. Amphiphillic styryl dyes such as FM1-43 bind to the plasma membrane and fluoresce. Following endocytosis, these properties allow FM dyes to be visualized as they are incorporated into vesicle membranes and effectively labeling active nerve terminals (Cochilla, Angleson, and Betz, 1999;Kavalali, Klingauf, and Tsien, 1999;Murthy, Sejnowski, and Stevens, 1997;Ryan, Reuter, Wendland, Schweizer, Tsien, and Smith, 1993). Upon activation of these FM1-43 stained synapses, the fluorescence decreases as the vesicles are exocytosed and the dye diffuses into the extracellular solution. Electrophysiological recordings of synaptic events from the postsynaptic cells yield aggregate activity measures from multiple synaptic terminals whereas fluorescent dye approaches allow assessments of individual release sites. In experiments employing FM1-43 the terminals are often loaded by depolarization with 45–90 mM extracellular [K^+] and then vesicle turnover tracked by measuring the loss of fluorescence during electrical field stimulation or depolarization with elevated extracellular K^+ (Klingauf, Kavalali, and Tsien, 1998;Ryan, Reuter, and Smith, 1997). Such dye studies reveal that some central terminals can have heterogeneous release probabilities and release may be different across neurons even within a single anatomical region (Murthy, Sejnowski, and Stevens, 1997;Waters and Smith, 2002) or by variation in modes of endocytosis (Harata, Choi, Pyle, Aravanis, and Tsien, 2006;Smith, Renden, and von, 2008).

The solitary tract nucleus (NTS) contains a diverse mix of afferent inputs and neuron phenotypes including 2nd order neurons which receive glutamatergic synapses originating from cranial visceral primary afferents that enter the brain via the solitary tract (ST) (Andresen and Kunze, 1994). The afferent heterogeneous mix arises from various visceral organs and contains two major subclasses - myelinated and unmyelinated (Doyle, Bailey, Jin, and Andresen, 2002;Jin, Bailey, Doyle, Li, Chang, Schild, Mendelowitz, and Andresen, 2003). Unmyelinated afferents extend central terminals into the NTS that can be distinguished by their expression of presynaptic capsaicin (CAP) sensitive TRPV1 receptors (Andresen and Peters, 2008;Bailey, Hermes, Andresen, and Aicher, 2006;Doyle, Bailey, Jin, and Andresen, 2002;Jin, Bailey, Doyle, Li, Chang, Schild, Mendelowitz, and Andresen, 2003;Jin, Bailey, Li, Schild, and Andresen, 2004). GABAergic inhibitory synaptic terminals also contact these same neurons and interact with afferent-released glutamate to modulate GABA release (Jin, Bailey, and Andresen, 2004). This inherent heterogeneity makes it particularly challenging to discern important aspects of the mechanisms governing vesicle release from these terminals within and across neurons.

In the present studies, we assessed synaptic transmission in NTS neurons by optical tracking of individual terminals in order to compare vesicle turnover properties with synaptic characteristics measured electrically. Neurons were isolated selectively from the medial sub nucleus of NTS. Using a micro-harvesting approach, we mechanically dissociated these cells and preserved native terminals without using potentially damaging enzymes such as trypsin or proteases (e.g. (Catacuzzeno, Fioretti, Perin, and Franciolini, 2003;Drewe, Childs, and Kunze, 1988;Kimitsuki, Ohashi, Wada, Fukudome, and Komune, 2005;Lee, Akaike, and Brown, 1977). Our studies reveal that CAP selectively and effectively destains a subset of terminals

while leaving adjacent CAP-resistant terminals fully stained on single neurons. Common destaining kinetic patterns across terminals provide evidence that individual CAP-sensitive terminals have similar, homogeneous release properties within this phenotype and in turn that solitary tract activated EPSCs arise from activation of multiple, very uniform terminals. Surprisingly, only relatively low concentrations of K^+ (10 mM) efficiently triggered synaptic release in these neurons and this suggests cautious use of conventional, much higher K^+ concentrations.

2. RESULTS

NTS neurons isolated with synaptic terminals

Our vibrating stylus dissociated neurons within a carefully delimited portion of medial NTS from horizontal brainstem slices (Jin, Bailey, Li, Schild, and Andresen, 2004) (Figure 1, dashed box). Neurons were micro-harvested generally from within the upper 50–100 μm of the slice surface. The neurons from the targeted region had appearances after isolation that generally resembled neurons commonly observed in slices (Figure 1C, D). The micro-harvested neurons often retained single processes exiting opposite poles of the soma so that individual somatodendritic terminals could be targeted for direct, optical study using the FM1-43 dye approach.

Punctate irregularities are synaptic terminals

Close examination of the surface of such dispersed NTS neurons showed small (~1–2 μm in diameter), punctate irregularities (Figure 2A, left) that were consistent with synaptic terminals. This localization was consistent with terminals identified previously in our electron microscopic studies of neurons in this region (Bailey, Hermes, Andresen, and Aicher, 2006). Likewise, antibodies to synaptophysin 1, a key synaptic vesicle membrane protein, yielded punctate staining in parallel experiments on these dissociated neurons. The synaptophysin 1 immunoreactive puncta were found distributed across the surface of the soma indicating synaptic specializations that extended along the primary processes (supplemental video clip Figure). Such puncta were similar in size, shape and distribution as the punctate irregularities observed under IR-DIC on live cells.

Puncta stain and destain with FM1-43

Following dye loading of live dispersed neurons with 4 μM FM1-43 plus 10 mM K^+, neurons displayed fluorescence co-localized at the punctate structures visible under IR-DIC (Figure 2A, middle panel). These FM1-43 stained puncta were similar in size and distribution to the cranial afferent terminals on NTS neurons labelled through anterograde transport of carbocyanine dye applied to peripheral afferent nerve trunks (Andresen and Peters, 2008;Doyle, Bailey, Jin, Appleyard, Low, and Andresen, 2004;Mendelowitz, Yang, Andresen, and Kunze, 1992). FM1-43 stained clusters of terminals and represent dye containing endocytosed vesicles (Figure 2A, middle panel). In most neurons, 2–4 dye loaded terminals could be monitored simultaneously. Electrophysiological recording from dispersed NTS neurons confirmed that most cells received both excitatory and inhibitory synaptic inputs. These synaptic events (Figure 2B) were distinguished by their rates of decay and sensitivity to specific antagonists (Jin, Bailey, and Andresen, 2004;Jin, Bailey, Li, Schild, and Andresen, 2004). Events during the control superfusion period with normal ACSF (Figure 2B) had slow decay times (~48 ms) and were IPSCs sensitive to the specific GABA antagonist, bicuculline (100 μM) while events with short decay times (~9 ms) were EPSCs blocked by glutamate antagonists (20 μM NBQX and 100 μM AP5). Thus, all cells likely have a mixture of at least two types of terminals containing either glutamate or GABA.

Inter-terminal destaining responses

To compare individual terminal characteristics, we stained neurons and measured destaining of FM1-43 during depolarization with elevated extracellular K^+. We selected focal planes within individual neurons that contained multiple puncta that could be tracked simultaneously. While fluorescence was relatively stable during the initial superfusion with normal ACSF, destaining with 10 mM K^+ ACSF followed similar time courses in most neurons evoking generally comparable destaining across all recorded terminals (Figure 3A). Destaining of nerve terminals was well described by an exponential decline with an average time constant of 84 ± 15 s (8 terminals) similar to that observed by others (Chen, Barg, and Almers, 2008;Gaffield and Betz, 2006;Harata, Pyle, Aravanis, Mozhayeva, Kavalali, and Tsien, 2001;Smith, Bergsman, Harata, Scheller, and Tsien, 2004;Waters and Smith, 2002). However, in other neurons (2/9), 10 mM K^+ evoked clearly different amounts of destaining of coplanar terminals (Fig. 3B). It might be expected that terminals populated by similar ion channels and releasing the same transmitter might have similar destaining characteristics and the converse – that diverse source neurons, e.g. glutamatergic afferents vs. GABAergic interneurons might have different release characteristics. This latter diversity (heterogeneity) also might include different neuron types within the afferent class of terminals.

Vesicle destaining homogeneous within TRPV1 phenotype

To address the potential for heterogeneous terminals within a single class of terminals, we tested the destaining pattern across terminals sharing a common pharmacological profile – those sensitive to the TRPV1 agonist capsaicin (CAP). Previous electrophysiological studies demonstrated that ST afferents can be divided by CAP sensitivity into two broad classes belonging to either slow conducting, C-type neurons with unmyelinated axons or rapidly conducting, myelinated (A-type) afferents (Jin, Bailey, Li, Schild, and Andresen, 2004). In dissociated NTS neurons, CAP reversibly increases the rate of glutamatergic sEPSCs identifying such neurons as 2^{nd} order with C-type terminals (Figure 4). After abruptly increasing, the rate of sEPSCs decreased after 30 seconds of exposure to CAP suggesting a limited number of vesicles available for release or terminal inactivation by receptor desensitization or depolarization block of voltage dependent ion channels (Figure 4).

We asked if vesicle destaining was different in the CAP-sensitive terminals. Terminals were identified following loading with FM1-43 using K (10 mM), had stable fluorescence levels during superfusion with normal ACSF and then destained with either 10 mM K^+ or with 100 nM CAP. A total of 23 NTS neurons were tested with CAP to destain FM1-43 stained terminals. In individual neurons, CAP destained some terminals but not others (Figure 5A). Note that the slow decline in fluorescence in the CAP-resistant terminals is similar to the pre-solution change period and thus consistent with bleaching as a result of the measurements (Figure 5A). In 7 CAP-sensitive neurons, a total of 11 synaptic terminals were CAP-sensitive and these terminals had remarkably similar destaining profiles to CAP (Figure 5A, B). Across all 23 NTS neurons, 29 terminals showed little destaining to CAP (Figure 5C) and represent CAP-resistant terminals. Five NTS neurons displayed a mix of terminals – CAP-sensitive and resistant. Note that not all terminals could be monitored simultaneously since they needed to be in the same plane of focus. Based on electrophysiological experiments (Figure 4 and (Jin, Bailey, Li, Schild, and Andresen, 2004)), CAP-sensitive terminals presumably arise from glutamatergic C-type cranial afferent terminals. Thus, the uniform destaining kinetics to CAP suggest that the release properties of individual C-type afferent terminals do not vary (Figure 5B). The results demonstrate that CAP is quite selective in its actions. However, the identity of the CAP-resistant terminals is ambiguous and might represent CAP-resistant glutamatergic terminals or terminals containing another transmitter such as GABA.

To ask whether vesicle destaining to CAP was different from K^+ destaining of the same CAP-sensitive terminals, we used a second dye, FM5-95. A number of terminals were identified following loading with FM1-43 using K^+ (10 mM) that overlie puncta on the DIC image (Fig. 6A, left and middle) and found that all terminals destained using K^+. After destaining and washing, the neurons were restimulated with 100 nM CAP in the presence of FM5-95 (8 μM). This red-shifted styryl dye allowed CAP-stained terminals to be clearly distinguished from CAP-resistant terminals containing residual FM1-43 (Fig. 6A, right). The time course of the destaining of the CAP-resistant and CAP-sensitive terminals in this cell evoked with 10 mM K^+ were similar although the degree of destaining varied (Fig. 5B). The findings suggest that CAP-sensitive and CAP-resistant terminal release properties are quite similar and destaining to CAP most likely results from depolarization itself.

K^+ sensitivity of isolated NTS neurons and terminals

In the course of these studies, we found that higher K^+ containing ACSF solutions produced inconsistent destaining responses. Solutions containing K^+ concentrations as high as 100 mM are commonly used to stain and destain synaptic terminals with FM1-43 (Gaffield and Betz, 2006). Brief exposure of dispersed NTS neurons to 90 mM K^+ ACSF produced irreversible swelling (Figure 7A). Tracking of destaining of FM puncta was disrupted by distortions in the shapes of such cells (Figure 7A) and, surprisingly, some terminals remained clearly stained after 15 min exposure to this highly depolarizing solution. Changes in cell shape prevented accurate and reproducible tracking of destaining of terminals. Exposure to 90 mM K^+ ACSF significantly (repeated measures ANOVA, $F_{2,11} = 12.1$, $P=0.001$) increased cell diameter by about 20% (Figure 7B) despite a constant osmolarity and these changes were not reversed by extended washing in normal ACSF (Tukey Multiple Comparison Procedures, $P=0.245$). The appearance of a pronounced nucleolus suggested cell death in these neurons following 90 mM K^+ ACSF. The 10 mM K^+, milder destaining solution used in most of our studies did not alter cell shape or diameter (Figure 7B, $p>0.05$).

To test the synaptic responses to different K^+ compositions of ACSF, we turned to electrical recordings. Exposure of NTS neurons to 10 mM K^+ ACSF consistently increased the frequency of pharmacologically isolated EPSCs or IPSCs in all neurons (Figure 8). Rather than further increasing the frequency of synaptic events, raising K^+ ACSF above 10 mM produced inconsistent responses across individual dispersed NTS neurons (Figure 8). Note that, while 10 mM K^+ reversibly increased EPSC activity, 90 mM K^+ ACSF in the same neuron often immediately and completely inhibited spontaneous EPSCs. Such paradoxical responses are opposite the expected increment in neurotransmitter release with terminal depolarization. This brief exposure was rapidly reversed on return to Control solution. Even 45 mM K^+ ACSF, on average, failed to increment neurotransmitter release (Figure 9A). Such paradoxical synaptic responses were not unique to glutamate terminals since 90 K^+ ACSF often decreased IPSC frequencies as well (Figure 8–9). In many neurons, 90 mM K^+ altered the spontaneous release rate for considerable periods of time despite returning to control solution (Figure 8). In 7 of 10 tested neurons, EPSC frequency decreased in 90 mM K^+ ACSF (Control, 0.38 ± 0.1 vs. 90 mM K^+ 0.1 ± 0.04 Hz, n=7, $p=0.01$). However, in all tested neurons, 10 mM K^+ ACSF reversibly increased EPSC frequency by about two fold (Figure 9A, n = 11, $p=0.01$). Similarly, 10 mM K^+ ACSF consistently increased IPSC frequency (Figure 8B, $p<0.01$). Similar to EPSCs, 90 mM K^+ ACSF failed to increment IPSC frequency (Figure 9B). Despite the inconsistent relationship between synaptic frequency and ACSF K^+, the holding current closely followed expectations of a membrane highly permeable to K^+ (Figure 9C).

3. DISCUSSION

Ultimately, the release of neurotransmitter results from a complex series of events occurring within small central synaptic terminals but few stages of this process can be directly measured. The mechanisms regulating release are most often assayed indirectly by for example measuring the frequency of postsynaptic events – EPSCs and IPSCs. These measures gauge the final result of a multi-step process taking place in the presynaptic terminal that culminates in vesicle release from multiple synaptic terminals and release sites. Here we measured vesicle turnover directly from single terminals of NTS neurons micro-harvested from the medial sub region and compared them to postsynaptic measures of that same presynaptic process - EPSCs and IPSCs. Our optical methods identified presynaptic specializations that were synaptophysin-positive and could be stained with the styryl dye FM1-43. Tracking the turnover of vesicle membrane of multiple individual terminals measured individual contributions to the overall synaptic release process. Our principal new findings include: 1. Identification of punctate structures visible on the surface of these isolated neurons that correspond to functioning presynaptic nerve terminals as measured with FM1-43. 2. Individual terminals on single neurons often responded to depolarization with generally similar vesicle turnover kinetics. 3. Capsaicin triggered vesicle turnover from a limited subset of terminals whose individual vesicle turnover characteristics were remarkably uniform. 4. The behavior of synaptic terminals on NTS neurons did not meet the assumptions for conventional depolarizing high K^+ conditions beyond 20 mM – a finding that offers a note of caution in such procedures.

Characteristics of synaptic terminals retained on dispersed NTS neurons

Inspection of the surface of dispersed neurons suggested small surface structures suspected as synaptic terminals and both staining for the synaptic protein synaptophysin and the accumulation/release of FM1-43 confirmed their synaptic nature. Neurons from this region of NTS of guinea pigs were some of the first dispersed neurons with synaptic terminals to be studied electrophysiologically and used enzymes and trituration (Drewe, Childs, and Kunze, 1988). In our studies, by observing several terminals simultaneously, the similarity of destaining profiles suggested that synaptic membrane release and turnover was generally similar in most cases. Thus, release triggered by generalized depolarization (K^+) could not distinguish glutamate vesicles from GABA vesicles nor could it identify the source of these terminals. In the case of glutamate release, synaptic terminals could arise from cranial visceral afferent terminations or from central neurons (e.g. NTS interneurons or neurons projecting to NTS from elsewhere)(Andresen, Doyle, Bailey, and Jin, 2004). Our recent studies of medial NTS neurons suggest that most neurons in this region are second order neurons directly contacted by solitary tract afferents that release glutamate but in addition we found that most of these second order neurons also receive other synaptic contacts from glutamatergic interneurons (McDougall, Peters, and Andresen, 2009). In the present studies, one subset of cranial visceral afferent terminals destained whether activated with CAP or K^+ and their destaining kinetics were quite similar. Our results suggest that phenotypically similar synaptic terminals have relatively uniform release characteristics across individual terminals – a finding that is difficult to assess through postsynaptic electrophysiological measures. Clearly, CAP-resistant terminals could arise from many other sources and likely included both GABA and glutamate terminals in our samples.

Electrical recordings in whole-cell mode collect synaptic currents from an entire neuron. As a result, synaptic events represent a mixture of contacts from potentially multiple sources. A unique aspect of NTS is the presence of the central terminations of peripheral primary afferent neurons. Evidence from both in vivo (e.g. (Andresen and Peters, 2008;Mifflin, 1996)) and in vitro slice studies (Andresen and Peters, 2008;Bailey, Appleyard, Jin, and Andresen, 2008;Doyle and Andresen, 2001;McDougall, Peters, and Andresen, 2009) suggests that the

majority of medial NTS 2nd order neurons receive input from a single cranial visceral afferent axon which divides to make multiple glutamatergic contacts. In such cases with a single afferent neuron source, greater homogeneity of terminals might result within single neurons. However, it is possible that individual terminals even if sourced from a single neuron could have different release properties across active zones (Murthy, Sejnowski, and Stevens, 1997;Waters and Smith, 2002). Quantal analysis of solitary tract to NTS transmission suggests that these single afferent axons branch to give rise to ~20 (range 5–33) individual contacts (Andresen and Peters, 2008;Bailey, Jin, Doyle, Smith, and Andresen, 2006;Peters, McDougall, Kellett, Jordan, Llewellyn-Smith, and Andresen, 2008) – only a small fraction of which were likely to be retained on our dissociated NTS neurons.

Limitations of high K^+ for synaptic studies of NTS neurons

Investigations of vesicle turnover with FM dyes often utilize high K^+ solutions (>70 mM) for loading and unloading terminals (Gaffield and Betz, 2006;Klingauf, Kavalali, and Tsien, 1998;Ryan, Reuter, Wendland, Schweizer, Tsien, and Smith, 1993). Higher K^+ concentrations are thought to more effectively destain FM1-43 from presynaptic terminals (Richards, Bai, and Chapman, 2005). The highest K^+ solutions are suggested to increase the likelihood that release neurotransmitter occurs through full vesicle effacement rather than transient fusions with the plasma membrane ("kiss and run") in which neurotransmitter is only partially released with vesicles rapidly re-entering the release cycle (Harata, Pyle, Aravanis, Mozhayeva, Kavalali, and Tsien, 2001;Smith, Renden, and von, 2008). In our experiments, K^+ concentrations of ACSF >10 mM resulted in depressed synaptic responses of both glutamate and GABA terminals. However, mild depolarizing conditions (10 mM K^+ ACSF) uniformly triggered sustained increases in the frequency of EPSCs and IPSCs as well as reproducible destaining profiles of individual terminals. Resting neuronal membrane potentials are often dominated by K^+ conductance (Hille, 2001) so that increasing external [K^+] in ACSF should depolarize terminals. A potential explanation for the paradoxical actions of K^+ ACSF containing >10 mM is that terminals on NTS neurons might be depolarized sufficiently to rapidly inactivate voltage-dependent Na^+ and Ca^{2+} channels thus reducing excitability. In studies of cultured nodose neurons (Pamidimukkala and Hay, 2001), FM1-43 tracking of membrane endocytosis using 90 mM K^+ ACSF appears to have been well tolerated as with exocytotic studies in cultured central neurons (Gaffield and Betz, 2006). Discharge studies of pressure activated aortic baroreceptors suggest that doubling extracellular K^+ concentration (9 mM in those experiments) substantially depressed their mechanical sensitivity and overall discharge decreased over time with exposure to such solutions (Andresen, Kuraoka, and Brown, 1979;Thoren, Andresen, and Brown, 1982). If the sensitivity of such peripheral sensory terminals is representative of the central terminals within NTS of these same neurons, then K^+ concentrations typically employed in styryl dye experiments should suppress excitability and thus synaptic release as we have observed in the present studies. We also considered that the acutely isolated neurons might be less tolerant of substantial sustained depolarization. Although this might explain swelling during prolonged exposure to high K^+ (Figure 7A), reversible decreases in EPSC frequency are more difficult to understand but might reflect inactivation of terminal ion channels or the release process (Figure 8).

Synaptic release properties of cranial visceral afferent terminals

Many 2nd order neurons within medial NTS receive ST afferent contacts that originate from a single axon that generates a large fused EPSC through multiple contacts that are either CAP-sensitive or CAP-resistant (Andresen and Peters, 2008;Doyle, Bailey, Jin, and Andresen, 2002). The implication of such a synaptic arrangement for the present studies is that the observed homogeneity across individual CAP-sensitive terminals likely reflects terminal branches arising from a single afferent neuron. Cranial visceral primary afferents show properties characteristic of two major afferent classes: unmyelinated, C-type and myelinated,

A-type afferents that are similar to the myelinated/unmyelinated cellular differences in somatic afferents (Andresen, Doyle, Bailey, and Jin, 2004;Andresen and Kunze, 1994;Kunze and Andresen, 1991). TTX-resistant Na^+ channels are exclusively present in C-type axon of sensory neurons and convey unique action potential characteristics (Roy, Reuveny, and Narahashi, 1994;Schild, Clark, Hay, Mendelowitz, Andresen, and Kunze, 1994;Schild and Kunze, 1997). Previous synaptic studies of NTS 2nd order neurons showed that TRPV1 and P2X3 agonists evoked release of glutamate differentially from different subsets of afferent terminals and appear to be expressed in a C-type / A-type selective fashion from the cell bodies of nodose afferent neurons to their central terminations (Jin, Bailey, Li, Schild, and Andresen, 2004). For brainstem reflex arcs that are initiated at NTS, myelinated and unmyelinated afferents activate reflexes with systematically different frequency dependent characteristics such as the arterial baroreflex (Andresen and Peters, 2008;Fan and Andresen, 1998;Fan, Schild, and Andresen, 1999;Mendelowitz, Yang, Andresen, and Kunze, 1992). Like the differential expression of TRPV1 on unmyelinated cranial primary afferents, the impact of these afferent neuron differences are unclear on driving synaptic release and the degree to which afferent properties impact overall reflex performance beyond NTS remains to be determined.

4. EXPERIMENTAL PROCEDURES

NTS slices

Hindbrains of male Sprague-Dawley rats (2–3 wks old, Charles River) deeply anesthetized with isoflurane were removed from a total of 83 animals for the study as described previously (Doyle and Andresen, 2001;Jin, Bailey, and Andresen, 2004). Multiple neurons dispersed from a single animal were often used for more than one experiment. Each brain was placed in ice cold artificial cerebrospinal fluid (ACSF) composed of (in mM): 125 NaCl, 3 KCl, 1.2 KH_2PO_4, 1.2 $MgSO_4$, 25 $NaHCO_3$, 10 dextrose, 2 $CaCl_2$, and bubbled with 95%O_2 / 5% CO_2 (Doyle and Andresen, 2001). A trimmed block of the medulla centered on the obex was thinly cut horizontally (150–170 μm thick) in cold (4°C) ACSF with a sapphire knife (Delaware Diamond Knives, Wilmington, DE, USA). These horizontal slices contained the ST in the same plane as the NTS (Figure 1A) and were identical to those used for characterization of ST synaptic transmission to NTS neurons in situ (Doyle and Andresen, 2001). All animal procedures were performed with the approval of the Institutional Animal Care and Use Committee at Oregon Health & Science University, were designed to minimize pain and discomfort, and conform to the guidelines of the National Institutes of Health publication “Guide for the Care and Use of Laboratory Animals”.

Mechanical dissociation device

A custom-made, micro-dissociation device was created using a linear motor and electronic control circuit from a commercial shaver (ES8023, Panasonic Corporation of North America, Secaucus, NJ, USA) to drive the oscillation of a polished glass stylus (Figure 1) pulled from borosilicate pipette glass (1.0 mm × 0.25 mm, A-M Systems, Inc., Carlsborg, WA, USA). After fire-polishing the final tip diameter was 100–120 μm. The stylus was held in place using a micropipette holder (Warner Instruments, LLC, Hamden, CT, USA) and mounted to one arm of the shaver blade attachment assembly. The holder-motor assembly was then mounted on a micromanipulator. Using an AC power supply (MTR 28, Wild Heerbrugg, Switzerland), the shaver control circuit drove the blade oscillation at excursion amplitude that was adjusted by varying the driving current. AC power was modified by addition of step-down resistors to avoid high voltage damage of the linear motor and to control the range of the oscillation amplitude.

Micro-harvesting medial NTS neurons and recording

Slices were incubated for 1–3 hrs at 31 °C in ACSF before mechanical dispersion. For dispersion, the brain stem slice was transferred to a recording chamber filled with standard

external solution (mM), 150 NaCl, 5 KCl, 1 $MgCl_2$, 2 $CaCl_2$, 10 HEPES and 10 glucose (pH was adjusted to 7.4 with Tris-base). Neurons were harvested from restricted portions of the medial sub nucleus of NTS underlying the area postrema as previously described (Jin, Bailey, and Andresen, 2004). The dispersion pipette was directed to portions of NTS medial to the visible solitary tract using a stereomicroscope and the oscillating tip was lowered to the surface. The pipette oscillated (30 Hz) horizontally with excursions of 100–300 μm. The oscillating pipette tip was slowly moved using the micromanipulator to circumscribe an area of the sub nucleus generally from the most caudal end of the fourth ventricle rostrally up to 500 μm and medial from the solitary tract to within 50 μm of the edge of the fourth ventricle. This targeted area is a region densely innervated by aortic baroreceptor terminals (Andresen and Peters, 2008;Doyle and Andresen, 2001). Neurons were dissociated from the upper 100 μm of the dorsal surface of the slices. The remainder of the slice was removed from the dish and the dispersed neurons were allowed to settle and adhered to the bottom of the dish within 20 min. This sub region contains second order neurons receiving both CAP-sensitive and CAP-resistant afferents from the solitary tract (Doyle, Bailey, Jin, and Andresen, 2002). Voltage clamp recordings were made with an Axopatch 2B amplifier and pClamp 8 software (Axon Instruments, Molecular Devices, Sunnyvale, CA, USA). Electrical measurements were performed using the nystatin-perforated patch recording at room temperature. Recording electrodes were filled with a solution composed of (mM): 50 KCl, 100 K gluconate, 10 HEPES and the solution pH was adjusted to 7.2 with Tris-OH.

Vesicle recycling tracked with styryl dyes

Slices were visualized with a conventional microscope Axioskop 2 FS2+, (Zeiss, Thornwood, NJ, USA) equipped with infrared and differential interference contrast (DIC) optics (Figure 1A). For electrophysiology and styryl dye experiments from dissociated cells, neurons were visualized using an inverted microscope (TE2000S; Nikon, Tokyo, Japan or IX70, Olympus, Center Valley, PA, USA) equipped with DIC and fluorescence optics with either a 100x oil (1.4 NA) or a 60x water (1.2 NA) immersion objective. Two styryl dyes were used in different experiments and the filter sets for FM1-43 and FM5-95 imaging compatible with FITC (excitationHQ480/30X, dichroic 505DLCP, and emitter E570LP, Chroma Technology, Rockingham, VT, USA) or Texas red (TXRED-4040B-OMF-ZERO, Semrock, Rochester, NY, USA), respectively. Images were captured using an ORCA-ER digital CCD camera (Hamamatsu, Hamamatsu, Japan) and Wasabi image acquisition software (Hamamatsu). Image analysis was performed with Wasabi or Image Analysis (Bergsman, Krueger, and Fitzsimonds, 2006) and IgorPro (Lake Oswego, OR, USA).

Staining, wash and destaining solutions were applied via rapid application via either a Y-tube system constructed from basic lab materials or a single capillary with a manifold that provided complete solution changes surrounding the recorded neurons within 20 ms (Murase, Ryu, and Randic, 1989). ACSF K^+ composition was altered in equimolar exchange for Na^+ for use in dye experiments as well as in miniature synaptic recording. In all studies, neurons were under constant flow conditions that included 5–10 min initially during which normal ACSF superfused the neurons and stability of controls were measured. The standard staining and destaining ACSF contained a K^+ concentration of 10 mM to depolarize terminals. Staining was accomplished by 90 sec exposure to 10 mM K^+ ACSF solution. The FM dye in most experiments used 4 μM FM1-43 (N-(3-triethylammoniumpropyl)-4-(4-(dibutylamino)styryl) pyridinium dibromide) followed by 90 s wash using a low Ca^{2+} ACSF (0.2 mM $CaCl_2$ and 4 mM $MgCl_2$) to minimize vesicle turnover during the wash period. In one more elaborate subset, a two stage protocol initially stained terminals with FM1-43 using 10 mM K^+ and were then destained with the same K^+ solution. In the second stage, the same neurons were restained using 100 nM CAP plus 8 μM FM5-95 (N-(3-trimethylammoniumpropyl)-4-(6-(4-(diethylamino)phenyl) hexatrienyl)pyridinium dibromide), and then destained with the same

K^+ solution. Thus, in this two stage protocol, the red-shifted FM5-95 could be detected simultaneously along with FM1-43.

Preliminary tests of medial NTS neurons revealed unusual responses to high K^+ typically recommended (Gaffield and Betz, 2006). Therefore, in a dedicated series of experiments, multiple ACSF K^+ concentrations were tested including 45, 70 or 90 mM. We assessed cell shape changes in a limited series of K^+ ACSF experiments by measuring the cell diameter of the minor axis of these ellipsoid neurons across time and solution changes.

The optimal plane of focus was identified before destaining tests as the plane in which more than one synaptic bouton was in focus. This preferred focal plane was used throughout the remainder of the experiment and solution changes. Terminal structures outside of this preferred focal plane were not analyzed. Fluorescent puncta were analyzed off line. Following FM staining, circular areas of interest were designated at the beginning of each experiment to include single putative synaptic boutons and these fixed areas of interest analyzed throughout each experiment. The level of fluorescence from each area of interest was divided by the value at that areas of interest for 30 sec of control measurements and expressed as the fluorescence relative to control (e.g. control fluorescence = 1.0).

Immunohistochemistry

To verify the synaptic attributes of puncta as putative synaptic terminals, isolated NTS neurons were fixed for 15 min with formaldehyde (4% v/v) in Dulbecco's Phosphate Buffered Saline (PBS in mM - 137.9 NaCl, 2.7 KCl, 1.5 KH_2PO_4, 8.0 Na_2HPO_4-$7H_2O$, Invitrogen, Carlsbad, CA, USA). After washing cells three times with PBS, blocking solution (PBS containing 1% bovine serum albumin and 2% normal goat serum) with triton X (0.1%) was added for 30 min at room temperature. The cells were then incubated with 1:200 mouse anti-synaptophysin 1 monoclonal antibody, mAb (Cat. No. 101 011, Synaptic Systems, Germany) diluted in the blocking solution overnight at 4°C. Alternatively, cells were incubated with 1:200 rabbit anti-synaptophysin 1 polyclonal antibody (Cat. No. 101 002, Synaptic Systems, Germany) diluted in the blocking solution overnight at 4°C. The mouse monoclonal anti-synaptophysin was directed against the SY38 epitope (Knaus and Betz, 1990) which is a pentapeptide repeat structure in the carboxy-terminal cytoplasmic tail of synaptophysin: 269 –289 YQPDYGQPASGGGGYGPQGDY. The rabbit polyclonal anti-synaptophysin 1 was directed against the synthetic peptide GPQGAPTSFSNQM (aa 301 – 313 in human synaptophysin 1). Following washing 3 times for 5 min each time with PBS, the cells were incubated with goat anti-mouse IgG AlexaFluor 488 (1:1000) diluted in blocking solution for 60 min, and washed 3 × 5 min with PBS. Coverslips were then mounted with Vectashield reagent (Molecular Probes/Invitrogen, Eugene, OR) with 1:80 diluted DAPI (4′,6-diamidino-2-phenylindole, Molecular Probes) to stain cell nuclei. Images were acquired by laser scanning confocal LSM 710 (Zeiss, Germany) using a Plan-Apochromat 63x/1.40 Oil DIC M27 objective. Pixel size was × 0.058 μm, y 0.058 μm, and z 0.399 μm (image size 512 × 512 × 38). The pinhole was 54 μm for detecting green fluorescence from AlexaFluor 488 and was 43 μm for blue fluorescence from DAPI. Tests for specificity of the secondary Ab omitted the anti-synaptophysin 1 mAb.

Data analysis and statistics

Decay time constants were calculated with a least squares fitting routine for a single decay exponential between the 10% and 90% peak amplitude using the graphical analysis software Origin 7.5 (OriginLab Corp., Northampton, MA, USA). Friedman repeated measures ANOVA on ranks (frequency, decay-time constant and amplitude) or a one-way, repeated measures ANOVA (baseline values, amplitude, latency and diameter) with post hoc pairwise multiple comparisons (Holm-Sidak method or Tukey, SigmaStat v3.5, San Jose, CA, USA). In one case,

the data set were not normally distributed and initial comparisons used the nonparametric, Kruskal-Wallis one way ANOVA on Ranks that was followed by pairwise multiple comparison procedures using the Dunn's Method. All data are represented as mean ± SEM and $p<0.05$ was considered statistically significant.

Drugs

Capsaicin, NBQX (2,3-dihydroxy-6-nitro-7-sulfamoyl-benzo[f]quinoxaline-2,3-dione), AP-5 (D-2-amino-5-phosphonopentanoate), bicuculline methylbromide, and gabazine (SR-95531, $GABA_A$ antagonist, 4-[6-imino-3-(4-methoxyphenyl)pyridazin-1-yl] butanoic acid hydrobromide) were obtained from Sigma-RBI (Natick, MA, USA).

Supplementary Material

Refer to Web version on PubMed Central for supplementary material.

Acknowledgments

Grants from the National Institutes of Health HL-41119 (MCA), HL-83115 (MCA, SMS), and NS-43444 (SMS) supported this work.

Abbreviations

ACSF	artificial cerebrospinal fluid
ANOVA	analysis of variance
CAP	capsaicin
EPSCs	excitatory postsynaptic currents
FM1-43	N-(3-triethylammoniumpropyl)-4-(4-(dibutylamino)styryl)pyridinium dibromide
FM5-95	(N-(3-trimethylammoniumpropyl)-4-(6-(4-(diethylamino)phenyl) hexatrienyl) pyridinium dibromide)
GABA	gamma aminobutyric acid
IPSCs	inhibitory postsynaptic currents
mAB	monoclonal antibody
NTS	solitary tract nucleus
ST	solitary tract
TRPV1	transient receptor potential vanilloid type 1
TTX	tetrodotoxin

Reference List

Andresen MC, Doyle MW, Bailey TW, Jin YH. Differentiation of autonomic reflex control begins with cellular mechanisms at the first synapse within the nucleus tractus solitarius. Braz J Med Biol Res 2004;37:549–558. [PubMed: 15064818]

Andresen MC, Kunze DL. Nucleus tractus solitarius: gateway to neural circulatory control. Annu Rev Physiol 1994;56:93–116. [PubMed: 7912060]

Andresen MC, Kuraoka S, Brown AM. Individual and combined actions of calcium, sodium and potassium ions on baroreceptors in the rat. Circ Res 1979;45:757–763. [PubMed: 498439]

Andresen MC, Peters JH. Comparison of baroreceptive to other afferent synaptic transmission to the solitary tract nucleus. Am J Physiol Heart Circ Physiol 2008;295:H2032–H2042. [PubMed: 18790834]

Bailey TW, Appleyard SM, Jin YH, Andresen MC. Organization and properties of GABAergic neurons in solitary tract nucleus (NTS). J Neurophysiol 2008;99:1712–1722. [PubMed: 18272881]

Bailey TW, Hermes SM, Andresen MC, Aicher SA. Cranial visceral afferent pathways through the nucleus of the solitary tract to caudal ventrolateral medulla or paraventricular hypothalamus: Target-specific synaptic reliability and convergence patterns. J Neurosci 2006;26:11893–11902. [PubMed: 17108163]

Bailey TW, Jin YH, Doyle MW, Smith SM, Andresen MC. Vasopressin inhibits glutamate release via two distinct modes in the brainstem. J Neurosci 2006;26:6131–6142. [PubMed: 16763021]

Bergsman JB, Krueger SR, Fitzsimonds RM. Automated criteria-based selection and analysis of fluorescent synaptic puncta. J Neurosci Methods 2006;152:32–39. [PubMed: 16198002]

Catacuzzeno L, Fioretti B, Perin P, Franciolini F. Frog saccular hair cells dissociated with protease VIII exhibit inactivating BK currents, K(V) currents, and low-frequency electrical resonance. Hear Res 2003;175:36–44. [PubMed: 12527123]

Chen X, Barg S, Almers W. Release of the styryl dyes from single synaptic vesicles in hippocampal neurons. J Neurosci 2008;28:1894–1903. [PubMed: 18287506]

Cochilla AJ, Angleson JK, Betz WJ. Monitoring secretory membrane with FM1-43 fluorescence. Annu Rev Neurosci 1999;22:1–10. [PubMed: 10202529]

Doyle MW, Andresen MC. Reliability of monosynaptic transmission in brain stem neurons in vitro. J Neurophysiol 2001;85:2213–2223. [PubMed: 11353036]

Doyle MW, Bailey TW, Jin YH, Andresen MC. Vanilloid receptors presynaptically modulate visceral afferent synaptic transmission in nucleus tractus solitarius. J Neurosci 2002;22:8222–8229. [PubMed: 12223576]

Doyle MW, Bailey TW, Jin YH, Appleyard SM, Low MJ, Andresen MC. Strategies for cellular identification in nucleus tractus solitarius slices. J Neurosci Methods 2004;37:37–48. [PubMed: 15196825]

Drewe JA, Childs GV, Kunze DL. Synaptic transmission between dissociated adult mammalian neurons and attached synaptic boutons. Science 1988;241:1810–1813. [PubMed: 2459774]

Fan W, Andresen MC. Differential frequency-dependent reflex integration of myelinated and nonmyelinated rat aortic baroreceptors. Am J Physiol Heart Circ Physiol 1998;275:H632–H640.

Fan W, Schild JH, Andresen MC. Graded and dynamic reflex summation of myelinated and unmyelinated rat aortic baroreceptors. Am J Physiol Regul Integr Comp Physiol 1999;277:R748–R756.

Gaffield MA, Betz WJ. Imaging synaptic vesicle exocytosis and endocytosis with FM dyes. Nat Protoc 2006;1:2916–2921. [PubMed: 17406552]

Harata N, Pyle JL, Aravanis AM, Mozhayeva M, Kavalali ET, Tsien RW. Limited numbers of recycling vesicles in small CNS nerve terminals: implications for neural signaling and vesicular cycling. Trends Neurosci 2001;24:637–643. [PubMed: 11672807]

Harata NC, Choi S, Pyle JL, Aravanis AM, Tsien RW. Frequency-dependent kinetics and prevalence of kiss-and-run and reuse at hippocampal synapses studied with novel quenching methods. Neuron 2006;49:243–256. [PubMed: 16423698]

Hille, B. Ionic channels of excitable membranes. Sinauer Associates; Sunderland, MA: 2001.

Jin YH, Bailey TW, Andresen MC. Cranial afferent glutamate heterosynaptically modulates GABA release onto second order neurons via distinctly segregated mGluRs. J Neurosci 2004;24:9332–9340. [PubMed: 15496669]

Jin Y-H, Bailey TW, Doyle MW, Li BY, Chang KSK, Schild JH, Mendelowitz D, Andresen MC. Ketamine differentially blocks sensory afferent synaptic transmission in medial nucleus tractus solitarius (mNTS). Anesthesiology 2003;98:121–132. [PubMed: 12502988]

Jin YH, Bailey TW, Li BY, Schild JH, Andresen MC. Purinergic and vanilloid receptor activation releases glutamate from separate cranial afferent terminals. J Neurosci 2004;24:4709–4717. [PubMed: 15152030]

Kavalali ET, Klingauf J, Tsien RW. Properties of fast endocytosis at hippocampal synapses. Philos Trans R Soc Lond B Biol Sci 1999;354:337–346. [PubMed: 10212482]

Kimitsuki T, Ohashi M, Wada Y, Fukudome S, Komune S. Dissociation enzyme effects on the potassium currents of inner hair cells isolated from guinea-pig cochlea. Hear Res 2005;199:135–139. [PubMed: 15574308]

Klingauf J, Kavalali ET, Tsien RW. Kinetics and regulation of fast endocytosis at hippocampal synapses. Nature 1998;394:581–585. [PubMed: 9707119]

Knaus P, Betz H. Mapping of a dominant immunogenic region of synaptophysin, a major membrane protein of synaptic vesicles. FEBS Lett 1990;261:358–360. [PubMed: 1690151]

Kunze, DL.; Andresen, MC. Arterial baroreceptors: Excitation and modulation. In: Zucker, IH.; Gilmore, JP., editors. Reflex Control of the Circulation. CRC Press; Boca Raton: 1991. p. 141-166.

Lee K, Akaike N, Brown AM. Trypsin inhibits the action of tetrodotoxin on neurones. Nature 1977;265:751–753. [PubMed: 859585]

McDougall SJ, Peters JH, Andresen MC. Convergence of cranial visceral afferents within the solitary tract nucleus. J Neurosci 2009;29:12886–12895. [PubMed: 19828803]

Mendelowitz D, Yang M, Andresen MC, Kunze DL. Localization and retention in vitro of fluorescently labeled aortic baroreceptor terminals on neurons from the nucleus tractus solitarius. Brain Res 1992;581:339–343. [PubMed: 1382802]

Mifflin SW. Convergent carotid sinus nerve and superior laryngeal nerve afferent inputs to neurons in the NTS. Am J Physiol Regul Integr Comp Physiol 1996;271:R870–R880.

Murase K, Ryu PD, Randic M. Excitatory and inhibitory amino acids and peptide-induced responses in acutely isolated rat spinal dorsal horn neurons. Neurosci Lett 1989;103:56–63. [PubMed: 2476693]

Murthy VN, Sejnowski TJ, Stevens CF. Heterogeneous release properties of visualized individual hippocampal synapses. Neuron 1997;18:599–612. [PubMed: 9136769]

Pamidimukkala J, Hay M. Frequency dependence of endocytosis in aortic baroreceptor neurons and role of group III mGluRs. Am J Physiol Heart Circ Physiol 2001;281:H387–H395. [PubMed: 11406507]

Peters JH, McDougall SJ, Kellett DO, Jordan D, Llewellyn-Smith IJ, Andresen MC. Oxytocin enhances cranial visceral afferent synaptic transmission to the solitary tract nucleus. J Neurosci 2008;28:11731–11740. [PubMed: 18987209]

Richards DA, Bai J, Chapman ER. Two modes of exocytosis at hippocampal synapses revealed by rate of FM1-43 efflux from individual vesicles. J Cell Biol 2005;168:929–939. [PubMed: 15767463]

Roy ML, Reuveny E, Narahashi T. Single-channel analysis of tetrodotoxin-sensitive and tetrodotoxin-resistant sodium channels in rat dorsal root ganglion neurons. Brain Res 1994;650:341–346. [PubMed: 7953703]

Ryan TA, Reuter H, Smith SJ. Optical detection of a quantal presynaptic membrane turnover. Nature 1997;388:478–482. [PubMed: 9242407]

Ryan TA, Reuter H, Wendland B, Schweizer FE, Tsien RW, Smith SJ. The kinetics of synaptic vesicle recycling measured at single presynaptic boutons. Neuron 1993;11:713–724. [PubMed: 8398156]

Schild JH, Clark JW, Hay M, Mendelowitz D, Andresen MC, Kunze DL. A- and C-type nodose sensory neurons: Model interpretations of dynamic discharge characteristics. J Neurophysiol 1994;71:2338–2358. [PubMed: 7523613]

Schild JH, Kunze DL. Experimental and modeling study of Na^+ current heterogeneity in rat nodose neurons and its impact on neuronal discharge. J Neurophysiol 1997;78:3198–3209. [PubMed: 9405539]

Smith SM, Bergsman JB, Harata NC, Scheller RH, Tsien RW. Recordings from single neocortical nerve terminals reveal a nonselective cation channel activated by decreases in extracellular calcium. Neuron 2004;41:243–256. [PubMed: 14741105]

Smith SM, Renden R, von GH. Synaptic vesicle endocytosis: fast and slow modes of membrane retrieval. Trends Neurosci 2008;31:559–568. [PubMed: 18817990]

Thoren PN, Andresen MC, Brown AM. Effects of changes in extracellular ionic concentrations on aortic baroreceptors with nonmyelinated afferent fibers. Circ Res 1982;50:413–418. [PubMed: 7060235]

Waters J, Smith SJ. Vesicle pool partitioning influences presynaptic diversity and weighting in rat hippocampal synapses. J Physiol 2002;541:811–823. [PubMed: 12068042]

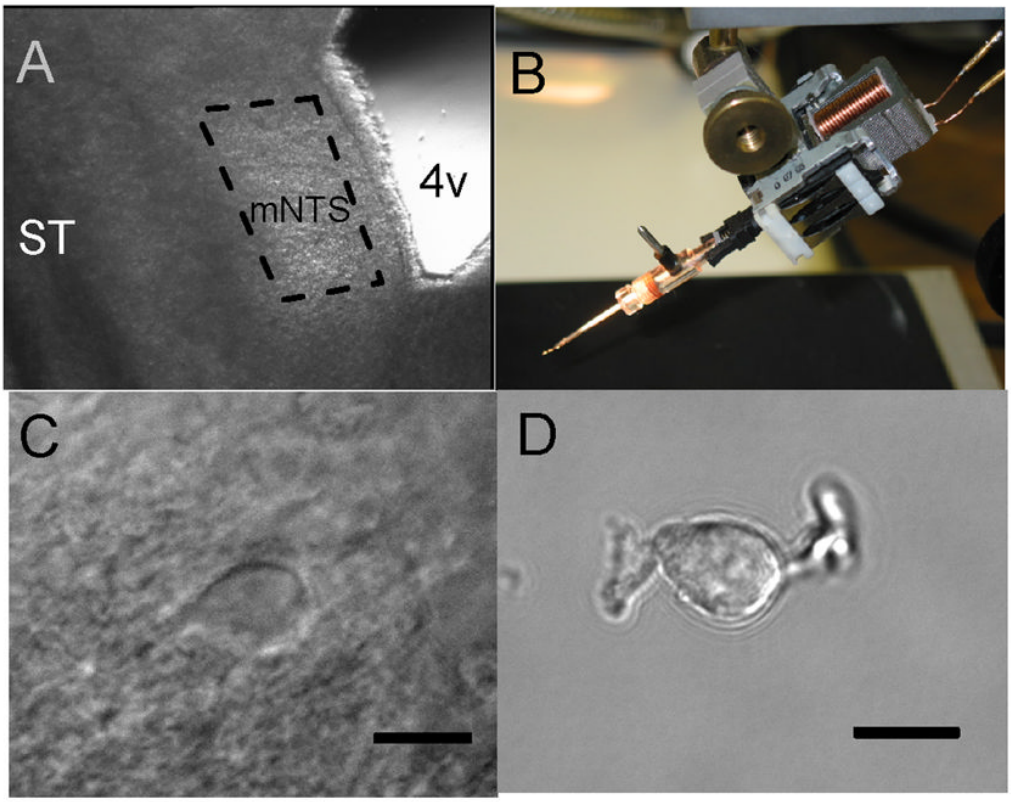

Figure 1.

The stylus method of mechanical dissociation allowed harvesting of neurons from delimited sub regions of horizontal brainstem slices without enzymes. **A**. Under low magnification (2.5×), a section of the medial sub nucleus of the NTS could be identified using anatomical landmarks within the left half of a horizontal brain stem slice (250 μm thick). Rostral is at the top of the micrograph and caudal is at the bottom. The selected sub region (broken line) was based on the rostral to caudal course of the solitary tract (ST) and the borders of the fourth ventricle (4V) with its caudal-most notch. **B.** The micromanipulator enabled these visible anatomical landmarks to guide careful placement and control of the tip of the vibrating stylus on the slice surface within the area of interest. Following multiple excursions of the vibrating stylus within this region, isolated neurons settled to the bottom of the dish. See details in **Methods. C.** Before dispersion, neurons within the slices typically appeared almond or spindle shaped with generally one major process at each pole of the neuron (40× objective) using infrared illumination and differential interference contrast (DIC) microscopy. **D.** Following dissociation, mechanically isolated neurons from medial NTS retained a general appearance similar to in situ neurons in slices and often retained short segments of proximal neural processes (60× objective). Bars = 10 μm. **C** and **D** are different neurons.

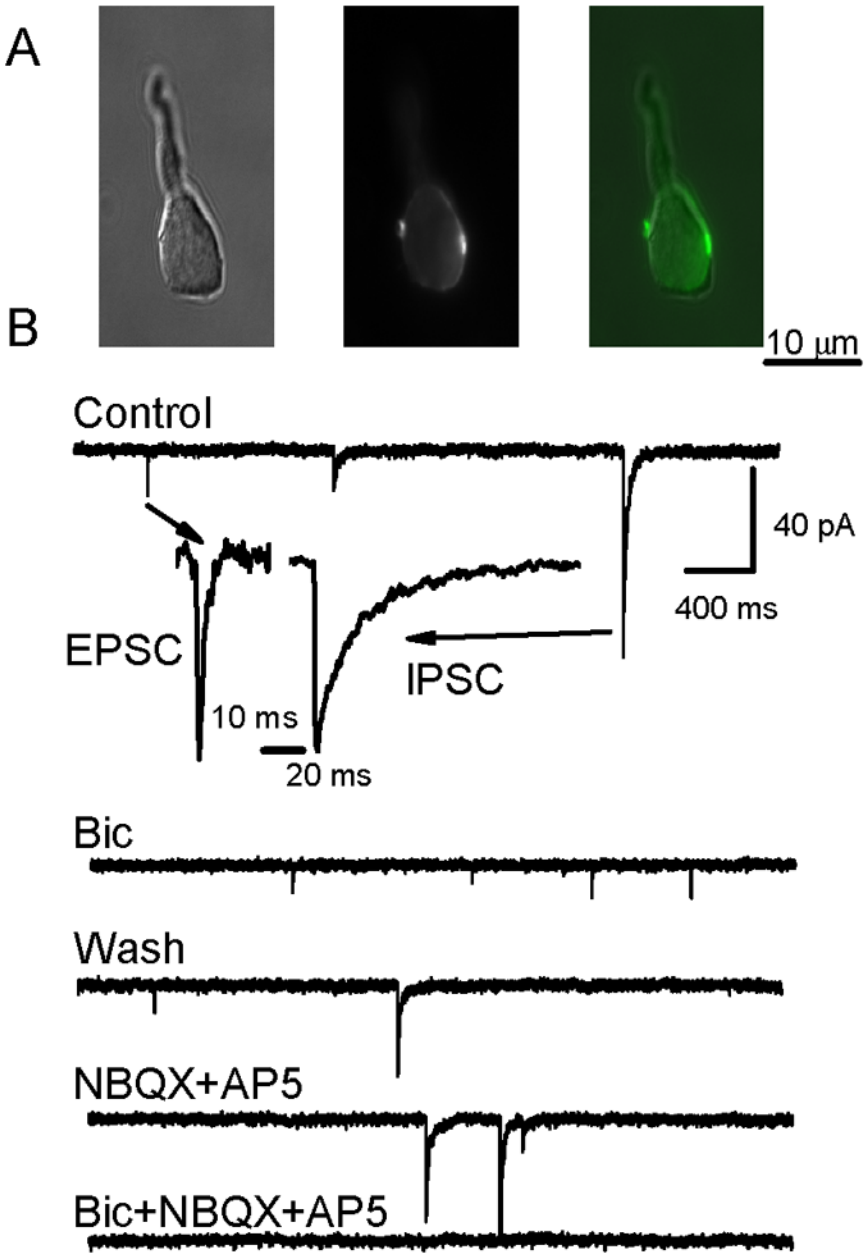

Figure 2.

Retained nerve terminals on acutely isolated NTS neurons are stained with FM1-43 and can be glutamatergic or GABAergic. **A**. Photomicrographs of a representative neuron (DIC image, left) that showed multiple fluorescent puncta (middle) along the edge of an NTS neuron cell body following loading of FM1-43 following loading using 10 mM external K^+ ACSF (center). Superimposition of DIC and epi-fluorescence images (right) shows two terminals on opposite sides of the neuron. **B**. In another representative isolated NTS neuron, whole cell currents were recorded with nystatin perforated patch electrodes and revealed the presence of two populations of synaptic events, small amplitude, fast spontaneous synaptic currents and larger amplitude, slow decaying synaptic currents. Insets show expanded traces normalized to the same peak current to illustrate that IPSCs had prolonged decay phases, whereas EPSCs rapidly returned to baseline. Note that neurons were superfused via the Y-tube system throughout the

experiment at constant flow and Control was normal ACSF. Bicuculline (100 μM) reversibly blocked large-amplitude, long-duration, synaptic currents and identified them as GABAergic IPSCs while preserving small-amplitude, brief synaptic currents (EPSCs). Wash with drug-free control solution restored the spontaneous IPSCs mixed with EPSCs. NBQX (20 μM) and AP5 (100 μM) blocked the fast events identifying them as glutamatergic EPSCs, but sIPSCs remained. All synaptic currents were blocked by combined bicuculline and NBQX.

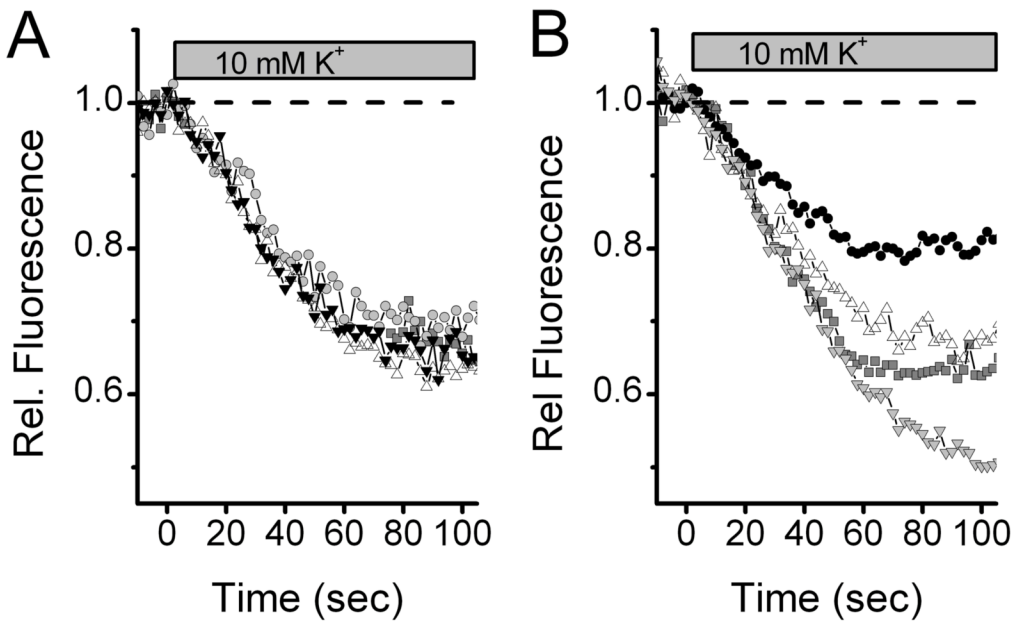

Figure 3.

Patterns of release kinetics differed somewhat across terminals within and across individual NTS neurons. Simultaneous tracking of 2–4 terminals allowed cross-terminal comparisons. Terminals in some neurons were quite homogeneous and in others substantially different. **A.** Multiple individual terminals identified using FM1-43 (4 μM) often had nearly identical destaining kinetics across all terminals. Note that fluorescence was relatively constant in the control period when cells were superfused with normal ACSF. Switch to 10 mM K^+ solutions promptly initiated destaining. The destaining profiles across four individual synaptic boutons were quite similar. **B.** In other neurons, however, substantially different destaining profiles were observed across multiple boutons on this single neuron within a single, simultaneous destaining cycle. Fluorescence was measured for 40 ms every 2 s. Symbols distinguish values from individual terminals across time through the 10 mM K^+ destaining sequence.

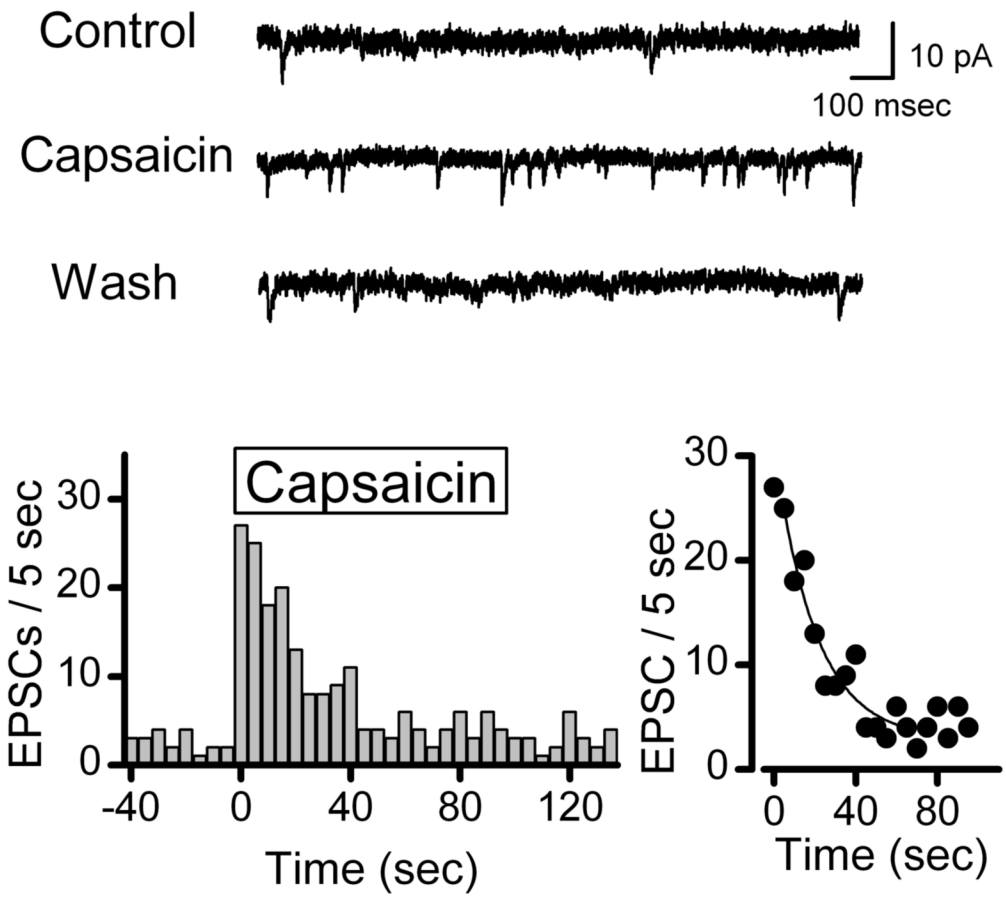

Figure 4.

The TRPV1 receptor agonist capsaicin (100 nM) could be used to evoke vesicle release selectively from unmyelinated cranial visceral afferent synaptic terminals. In some isolated NTS neurons, exposure to the TRPV1 receptor agonist capsaicin reversibly increased the frequency of spontaneous EPSCs above that observed during superfusion with normal ACSF (top panel). Introduction of capsaicin rapidly triggered a transient increase in the rate of EPSCs (lower left panel) which followed by a monoexponential decline in frequency (tau = 23 sec in this example, lower right panel). Counts of EPSC events were collected over time bins of 5 sec. The 10–90% fit (Origin software y = A1*exp(−x/t1)+ y0, $y0 = 2.8 \pm 2.9$, $A1 = 28.1 \pm 3.4$, $t1 = 20.3 \pm 7.6$ sec, $R^2 = 0.89$). In other neurons, EPSCs were unaffected by capsaicin – i.e. capsaicin-resistant EPSCs (not shown). Bicuculline was present in all experiments.

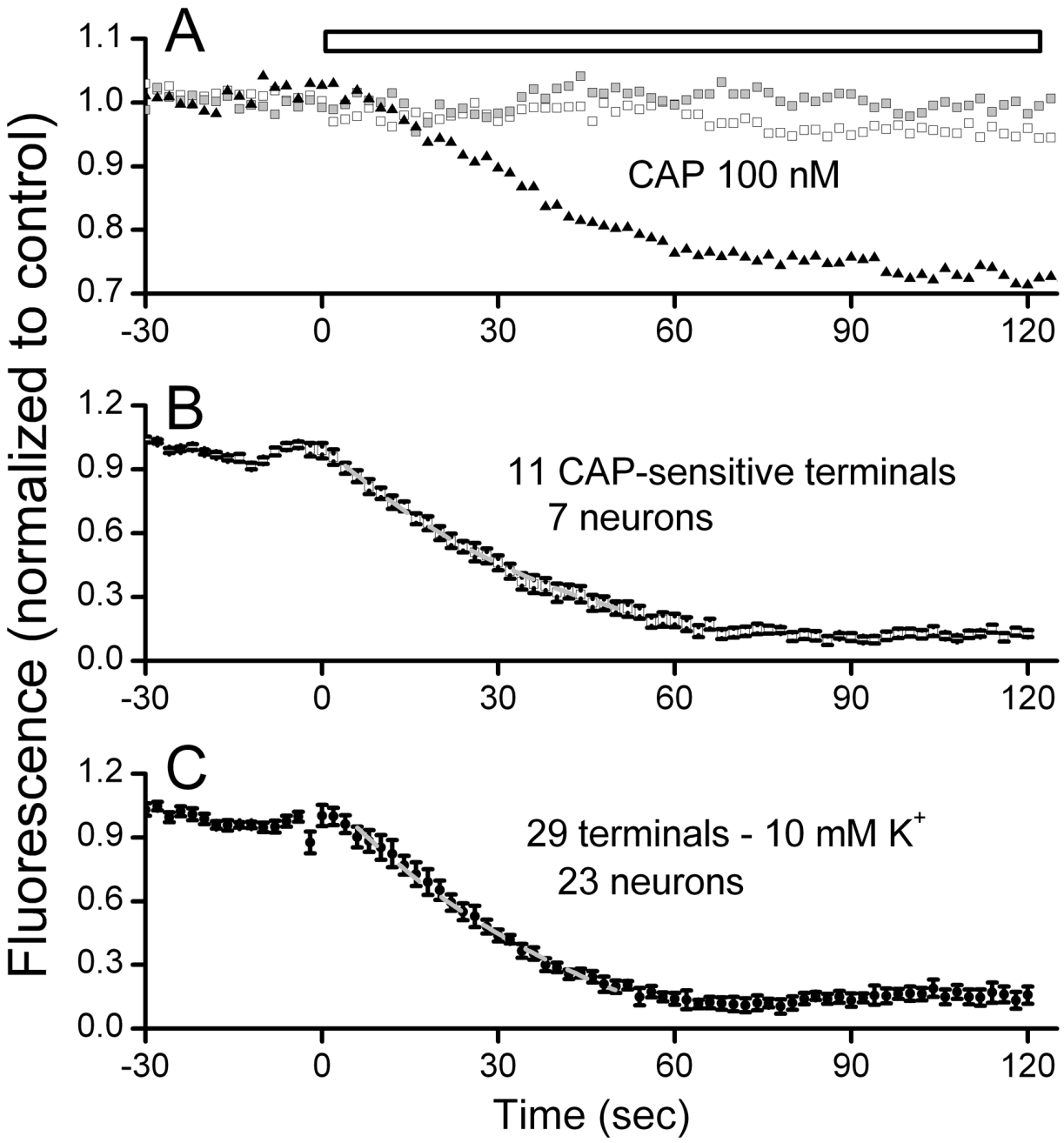

Figure 5.

Capsaicin (CAP) selective destaining of FM1-43 loaded terminals (4 μM). In a representative CAP-sensitive neuron (**panel A**), all terminals showed relatively constant fluorescence during superfusion with normal ACSF but only one of three monitored terminals was destained by exposure to 100 nM CAP. Each trace represents a single terminal whose fluorescence was periodically sampled through this single CAP exposure (**panel A**). The capsaicin-resistant terminals showed fluorescence declines similar to non-drug controls (results not shown) and during capsaicin followed a nearly linear trajectory of slow decline established during the control period (left-most portions of all traces). Thus, vesicle turnover was increased during CAP and CAP selectively destained some terminals and not others within the same neuron

(**panel A**). Single experiments were averaged across neurons for dye destaining of NTS neuron terminals sensitive to CAP (**panel B**) and to 10 mM K^+ (**panel C**). Data were fit between 10% and 90% of initial levels by a least squares method to a single exponential decay function. The average CAP-induced destaining curve represents 11 CAP-sensitive terminals from seven neurons from 7 animals using 100 nM CAP with a mean fit of y0 = −0.11 ± 0.11, A1=1.12 ± 0.10, t1=43.43 ± 8.48, R^2 = 0.99. Lower panel depicts the average for 10 mM K^+ destaining of 29 terminals from 23 neurons from 23 animals. Note that time courses of destaining are generally similar. Values mean ± SEM. These destaining time courses are quite similar to CAP-sensitive responses in sEPSCs (Figure 4). 10 mM fit was K, y0 = 0.73 ± 0.07, A1=1.44 ± 0.18, t1=48.3 ± 13.36, R^2 = 0.99

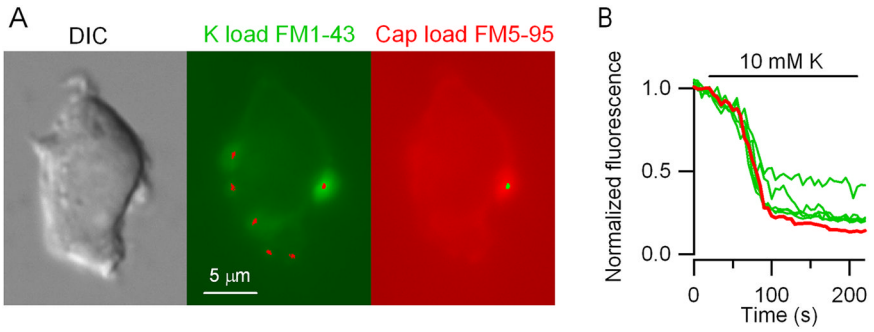

Figure 6.

Capsaicin staining of subsets of K-sensitive terminals. CAP-resistant and CAP-sensitive terminals destain to K^+ with similar kinetics. **A**, image of single NTS neuron in DIC (left) and following FM1-43 loading with 10 mM K^+ (middle). Six puncta (middle panel, red markings) were identified as areas of interest using automated analysis (Bergsman et al, 2005) within this single focal plane. Only one of six puncta stained with FM1-43 following K load remained visible after CAP and it destained with a similar time course in response to 10 mM K^+. **B**, Multiple individual terminals were destained of FM1-43 using 10 mM K^+ (green traces). Following this destaining, a different dye, FM5-95, was load using 100 nM CAP and analysis identified a single dyed terminal (green markings, **Panel A**, right). Repeat of 10 mM K^+ exposure destained the CAP-loaded terminal (red trace). Note that the kinetics of 10 mM K^+ destaining of FM1-43/FM5-95 in the CAP-sensitive terminal (red trace) was similar to CAP-resistant (green curves) puncta. Calibration bar represents 5 μm.

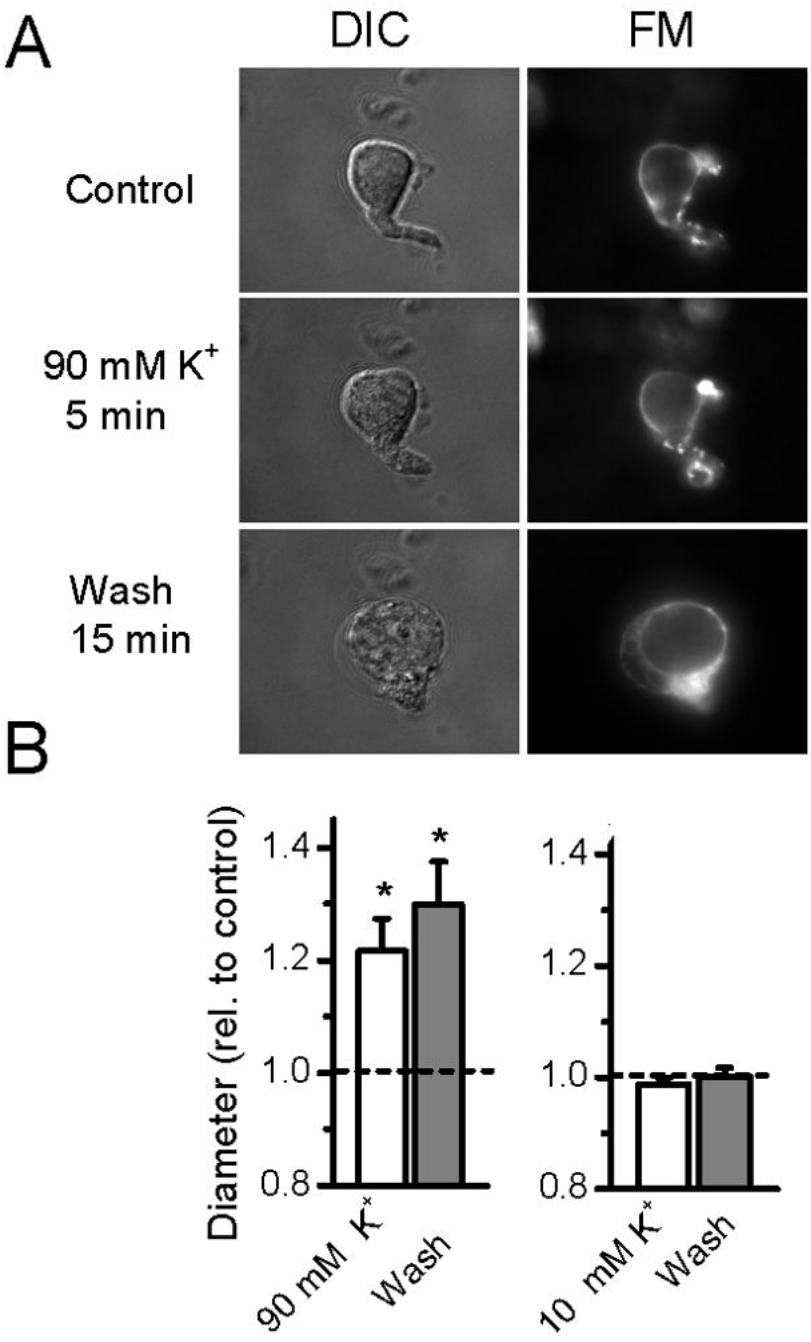

Figure 7.

Conventional staining/destaining with FM1-43 often employs quite elevated levels of K^+ that produced irreversible swelling in dispersed NTS neurons. **A**. Examples of photomicrographs of a representative neuron (from top to bottom) loaded using FM1-43 in combination with 45 mM K^+ ACSF, followed by 5 min destaining using a 90 mM K^+ ACSF, and a wash period of 15 minutes in normal (5 mM K^+) ACSF. DIC photomicrographs were taken using differential interference contrast enhancement and FM shows the epifluorescence from the same neuron. DIC and FM photomicrographs taken within 10 s of each other at the end of each treatment period. Note the progressive "rounding" out of the cell soma in the middle and lower panels and the pronounced blebbing and irregularities that are particularly evident in the Wash period.

The focal plane was fixed throughout this series of measurements. Some FM1-43 stained puncta evident at the end of the Control period remained bright despite 15 minutes exposure to 90 mM K^+ ACSF (compare FM Control and middle panel). Diameter continued to increase upon washing in control solution. The obvious shape changes and "rounding up" of neurons was striking and never occurred with milder, 10 mM K^+ ACSF treatments. **B.** On average, cell diameter increased after 90 mM K^+ treatment (Con vs. 90 mM K^+, paired T-test, p=0.018, n=13 from 10 animals) and on average continued to swell even following return to control solution (Wash). In separate experiments, no changes in diameter were found during 10 K^+ exposure or subsequent wash ($p>0.05$, n=6 from 6 animals). All data normalized for display relative to individual basal control before averaging. Broken line indicates control value of 1.0.

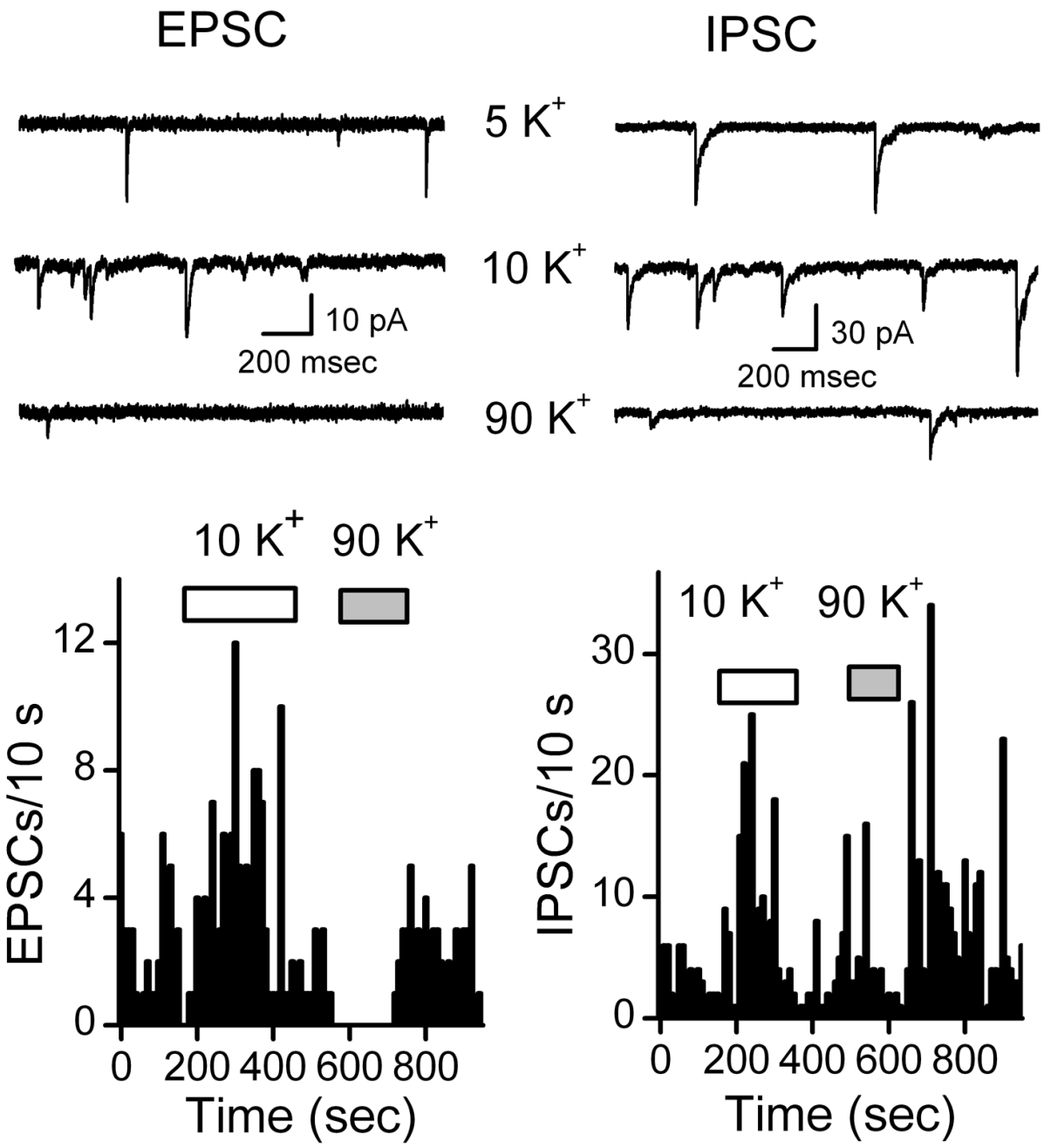

Figure 8.

Representative examples of electrophysiological responses to changing extracellular K^+ content of the ACSF perfusion solution on spontaneous synaptic activity in dispersed NTS neurons recorded using nystatin perforated patch electrodes. EPSCs isolated using gabazine (3 μM) were rapidly activated by switching from 5 mM (control) to 10 mM K^+ ACSF solution using the Y-tube (left panel). In the same neuron following return to control solution and activity, 90 mM K^+ ACSF immediately and paradoxically inhibited spontaneous EPSCs. This brief exposure was rapidly reversible on return to Control solution. Likewise spontaneous IPSCs were isolated using the inotropic glutamate receptor antagonists NBQX (20 μM) and AP5 (100 μM) (right panels). 10 mM K^+ ACSF solution effectively increased GABA release

whereas 90 mM K^+ ACSF decreased spontaneous IPSCs. Note that for the period following the 90 mM K^+ exposure, IPSC activity increased substantially above baseline activity after return to control solution. Note that cells were constantly superfused throughout these records with normal ACSF in the unmarked periods between horizontal bars. Holding potential was −60 mV and original traces for EPSCs and IPSCs are shown from different representative NTS neurons.

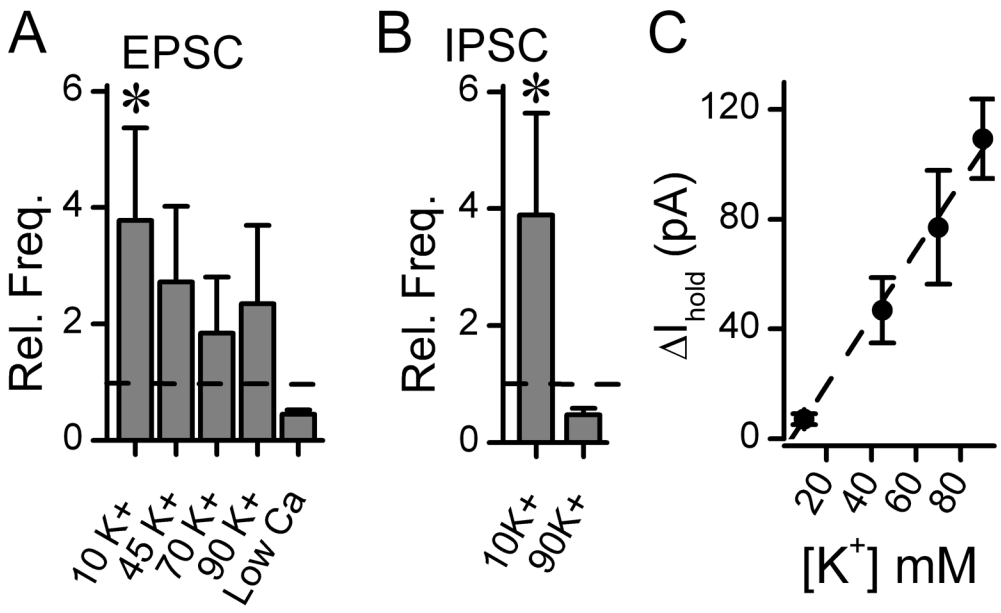

Figure 9.

Summary of changes in synaptic and holding currents in response to changes in extracellular K^+ in ACSF. **A.** Spontaneous EPSCs were isolated pharmacologically by gabazine (3 μM). Switching from perfusion with control (5 mM) to 10 mM K^+ ACSF increased EPSC frequencies [Chi-square$_1$= 14.00 (n=14), p=0.001, from 12 animals]. Greater changes in extracellular K^+ did not significantly change EPSC frequency from their respective controls (45 mM, $F_{1,6}$ =4.62, P=0.08; 70 mM,, $F_{1,10}$ =2.27, P=0.163; 90 mM, Chi-square$_1$= 1.60 (n=10), p=0.344, from 10 animals). Normally distributed datasets tested by Repeated measures ANOVA but where the Normality test failed, differences were tested with Repeated Measures ANOVA on Ranks and expressed as Chi-square. Low Ca^{2+} ACSF contained 0.2 mM $CaCl_2$ and 4 mM $MgCl_2$.and produced no significant change from control $F_{1,2}$ =0.00066, P=0.982 by ANOVA. Comparisons across samples used Kruskal-Wallis One Way Analysis of Variance on Ranks as data were not normally distributed and indicated significant differences among the ranked medians [H_3=8.16, (n=10) P=0.043]. The ranked medians indicated that the median value for 90 mM K^+ was significantly less than 10 mM (Dunn's Method for Multiple Comparison Procedures (Difference in Ranks = 12.87, Q=2.764, P=0.05). **B.** Spontaneous IPSCs were isolated pharmacologically using NBQX (20 μM) and AP5 (100 μM). Switching from perfusion with control (5 mM) to 10 mM K^+ increased IPSC frequencies (n=7, p<0.01, from 7 animals) but in 90 mM K^+ ACSF IPSC frequency decreased to near control (n=9, p>0.05, from 9 animals). Broken lines indicate Control levels of spontaneous synaptic activity levels normalized to 1.0. EPSC and IPSC amplitudes were unaltered by these solution changes suggesting that the changes acted presynaptically to alter event frequency. * indicates p <0.05. **C.** Graded changes in ACSF K^+ concentration were directly reflected in the holding currents (n = 6–8 neurons from 12 animals). Broken line is least squares linear regression fit (y= 7.32 – 1.20 x, r^2 = 0.55).